

Investigation of Optical Characteristics and Synthesis of Cobalt-Doped CdS (CdS:Co) Using Simple and Rapid Microwave Activated Method

R. Ranjan^{1*}, C.M.S Negi², K.P Tiwary³

¹Department of Electronics and Communication Engineering, Birla Institute of Technology Mesra, Patna Campus, Patna-800014, India.

²Department of Physical Sciences, Banasthali Vidyapith-304022 (Rajasthan), India.

³Department of Physics, Birla Institute of Technology Mesra, Patna Campus, Patna-800014, India.

Email id: rajeevraj@bitmesra.ac.in¹, nchandra@banasthali.in², kptiwary@bitmesra.ac.in³

***Orcid id:** 0009-0003-8440-0078

Abstract

Cobalt-doped cadmium sulphide semiconductor nanoparticles (CdS: Co NPs) were made using a microwave-assisted method with different cobalt concentrations. Chemicals like sodium sulphide, cobalt chloride, and cadmium acetate were used. The Debye-Scherrer equation helped find the nanoparticles' size, revealing a 2 to 4 nm range. X-ray diffraction showed a zinc-blend structure. The optical bandgap energies were found to be undoped and doped are 2.44eV and 2.58eV, respectively. For pure CdS, the XRD spectra display three main peaks at $2\theta = 26.68^\circ$, 44.16° , and 52.32° . Modest alterations have been noted in 2θ for Co doping levels of 3% in CdS NPs. The peaks point to the samples' cubic structure and correlate to the (1 1 1), (2 2 0), and (3 1 1) planes. The sizes of the nanoparticles, which are 2.29 nm, 3.44 nm, for pure and Co (3%) doped CdS, were determined using the FWHM and Debye Scherrer equation. The substitution of Co^{2+} ion for Cd^{2+} ion may be the cause of the decrease in nanoparticle size observed in the Co-doped CdS sample as concentration rises. The difference in the ionic radii of Cd^{2+} (0.98 Å) and Co^{2+} (0.72 Å) shows that when the concentration of Co-doped CdS increases, the lattice constant falls. The peak at 3646 cm^{-1} in the higher energy area of the $400\text{--}4000\text{ cm}^{-1}$ FTIR spectra is attributed to the O–H stretching of absorbed water on the surface of CdS. Its bending vibration confirms the existence of water.

Keywords: Co-doped CdS nanoparticles, X-ray diffraction, FTIR Spectra analysis, HRTEM

1. Introduction

Semiconductor materials have numerous applications in the structural, optical, chemical, and electro-catalytic domains because of their unique size, space, and structure [1-3]. Cadmium sulfide, or CdS, is a well-known compound semiconductor that finds widespread application in numerous significant fields, including molecular pathology, drug administration, photovoltaic cells, biosensing, bioimaging, and bio-molecular detection. All these uses are made possible by CdS's large band gap,

high photosensitivity, and photoconductivity [4]. The best-used dilute magnetic semiconductors (DMS) are two-VI quantum dot semiconductors (CdSe, ZnS, CdS, etc.), in which the host cations have been substituted with other elements (e.g., Cr, Co, Mn, and Fe). The interplay between the spin-induced magnetic moments of the transition metal ions and the host semiconductor lattice is responsible for these special characteristics [5]. A semiconductor with strong optical absorption

properties in the visible light spectrum is cadmium sulfide, or CdS. The direct band gap at room temperature is 2.42 eV. Cadmium sulfide is thus used in a few photonic devices, including lasers, photovoltaic systems, light-emitting diodes, and photo detectors [6-9]. Therefore, cadmium sulfide has been modified according to the requirements of the application. II-VI compound semiconductor nanoparticles have been applied in a wide range of fields recently, including sensors, the petrochemical industry, environmental clean-up, agriculture, biochemical applications, purification/water distillation, electronics, medical, and electrochemical industries [10].

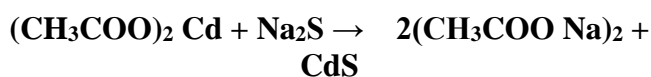
2. Experimental Analysis

2.1 Materials Required

All dilutions and sample preparation were done with distilled water. The analytical quality chemical reagents used in the synthesis process were not further purified before use. Cadmium acetate ($(\text{CH}_3\text{COO})_2\text{Cd}\cdot\text{H}_2\text{O}$), Cobalt chloride ($\text{CoCl}_2\cdot x\text{H}_2\text{O}$), and sodium sulfide ($\text{Na}_2\text{S}\cdot x\text{H}_2\text{O}$) were used as precursors. The glassware used in the experiment was dried after being cleaned with acid to get rid of any impurities.

2.2 Synthesis of Co-doped CdS nanoparticles

A stoichiometric mixture of aqueous cobalt chloride [$\text{CoCl}_2\cdot 4\text{H}_2\text{O}$] and aqueous cadmium acetate [$(\text{CH}_3\text{COO})_2\text{Cd}\cdot \text{H}_2\text{O}$] was mixed to prepare Co doped CdS nanoparticles in aqueous medium. First, sodium sulphide and cadmium acetate were used to create pure CdS nanoparticles in an aqueous media.



Next, we have made solutions with 3% cobalt by dissolving the specified amount of $\text{CoCl}_2\cdot 2\text{H}_2\text{O}$ in distilled water. Then, we have mixed cadmium acetate solution with the appropriate amount of $\text{CoCl}_2\cdot 2\text{H}_2\text{O}$ solution and stir the mix at up to 1000 rpm until it's evenly blended. Slowly, we have added sodium sulphide solution to the mix, and as the solution turns yellowish orange, it indicates the

formation of cobalt-doped CdS nanoparticles.

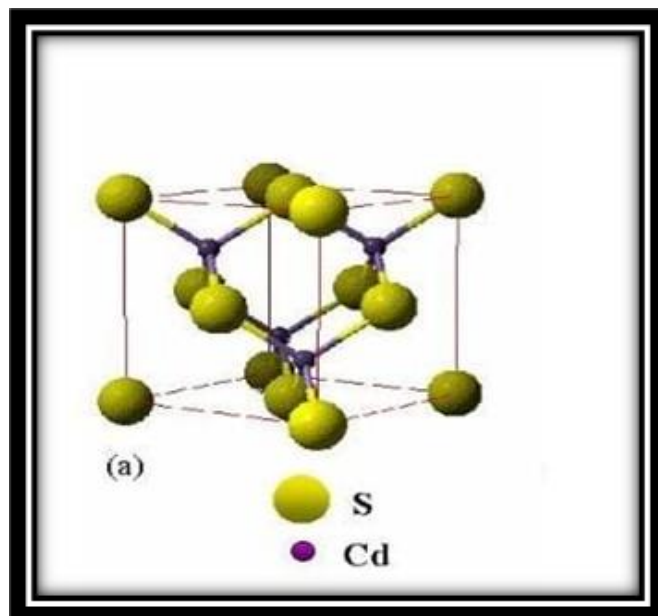


Figure 1 Structure of CdS

The solution was microwave irradiated for a precise amount of time and relaxed for a certain amount of time, creating a duty cycle of $t_1/(t_1+t_2)$, where one full cycle was created by irradiating the solution for 20 seconds and then relaxing it for the next 60 seconds. After 15 cycles, the resulting yellowish colloidal solution was collected. The resulting solution obtained after microwave process; it was filtered using filter paper which will be then kept in oven for 20 hours thus obtaining required nanoparticles. To delve into the characteristics of cobalt mixed CdS nanoparticles, we have employed UV Visible spectroscopy to record absorption spectra between 200-800 nm. The structural features of both undoped and doped CdS nanoparticles were scrutinized through XRD analysis. Further insight into the synthesized transition metal-doped CdS nanoparticles are gained using FTIR Spectra in the 400-4000 cm^{-1} range. CdS nanoparticles, renowned for their optical properties, find application in bio-labs for tissue and cell labelling. The fluorescence properties, pivotal for biomarker investigation, have been studied using UV-visible spectroscopy. Notably, the band gap of CdS: Co have been obtained by Tauc plot for a comprehensive analysis

of the produced nanoparticles with pure CdS and various dopants [11].

3. Result and discussion

3.1 X-RAY Diffraction (XRD)

Co-doped CdS nanoparticles as produced have had their structural properties analyzed using XRD analysis. This method can provide dimensions for individual cells and is widely used for phase identification. X-ray technique is also utilized to identify unidentified crystalline minerals. The Co-doped CdS nanoparticles' primary peaks can be detected at $2\theta = 26.52^\circ$, 43.8° , and 51.9° , which correspond to the (1 1 1), (2 2 0), and (3 1 1) planes. Using the Debye-Scherer equation, the average crystallite size was determined at the diffraction peaks' full-width half maximum

(FWHM):

$$D = k\lambda / \beta \cos\theta \quad (1)$$

Where,

k = particle shape factor (taken 0.9)

λ = X-Ray wavelength (1.5418 \AA)

β = FWHM value

θ = angle of diffraction

The inter planer spacing d can be calculated using

Bragg's law:

$$n\lambda = 2d \sin\theta \quad (2)$$

where,

λ = X-Ray wavelength (1.5418 \AA)

d = the inter planer spacing

θ = the angle of diffraction

$$d = a / \sqrt{(h^2 + k^2 + l^2)} \quad (3)$$

The other important structural parameter is calculated via the following equations:

$$\text{Microstrain, } \epsilon = \beta \cos\theta / 4 \quad (4)$$

$$\text{Dislocation density, } \delta = 1/D^2 \quad (5)$$

XRD Results

We also noticed that a slight shift of the XRD peaks toward lower 2θ diffraction angles in the XRD patterns of all Co: CdS as shown in Figure 2,

compared to pure CdS indicating an increase in the lattice parameters, and expansion in the unit cell volume of the CdS. Since the ionic radii of Co^{2+} (0.72 \AA) ions are less than that of Cd^{2+} (0.92 \AA) ions, the substitutional incorporation of Co^{2+} ions for Cd^{2+} sites or interstitial incorporation of Co^{2+} in the CdS host lattice cause a shift of XRD peaks to lower diffraction angles and lead to the expansion of volume of the unit cell. Therefore, a shift in the XRD peaks toward lower angle for higher Co doping concentration.

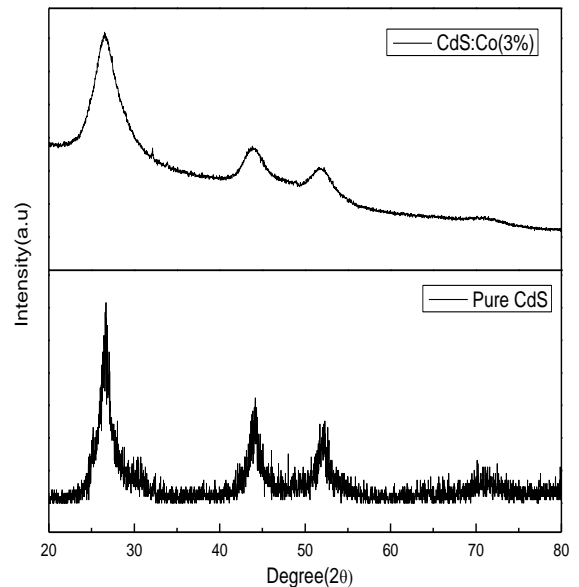


Figure 2 XRD Analysis Of Pure CdS&CdS:Co (3%)

FTIR Spectroscopy

The FTIR Spectra recorded from 400 to 4000 cm^{-1} at room temperature was used to identify the various functional and vibrational groups present in the synthesised sample of Co doped CdS nanoparticles in fig 3. The weak absorption band between 3400 and 3600 cm^{-1} is caused by the presence of moisture in the produced sample as well as OH stretching vibrations of water molecules. C-H stretching results from absorption peak between 2800 and 2900 cm^{-1} . The presence of H-O-H bending vibrations in water molecules accounts for the moderate and faint signal at 1550 cm^{-1} . The stretching vibration of the sulphate group could be

the reason for the medium-strong band orientation in the 1000–1150 cm^{-1} range.

UV-visible spectroscopy

The optical properties of the synthesized sample were examined using a room-temperature UV-visible spectrophotometer with a 200 nm to 800 nm wavelength range. Figure 4 shows the optical absorption spectra and band gap estimate of Co (3%) doped CdS nanoparticles. The bandgap is calculated by extrapolating the graph of $(\alpha h\nu)^2$

versus $h\nu$ as shown in Fig.4. By extrapolating the straight line to the X-axis, the band gap value is determined (in eV). The optical band gap of Co (3%) doped CdS is determined to be 2.68eV. The optical band gap of Co-doped CdS nanoparticles is clearly greater than that of bulk CdS. The band gap is found to increase from undoped to 3%, Co-doped. This is due to the quantum size effect of nanoparticles. The resulting band gap values coincide with the fact that the band gap increases as crystallite size also increases.

Table Different Parameters (Interplanar Spacing, Lattice Constant, Volume, Micro Strain, Dislocation Density, Average Crystallite Size) Of Mn-Doped Cds Nanoparticles

Compound	Peaks	2-theta (deg)	Interplanar spacing 'd' (ang)	FWHM (rad)	Lattice Constant 'a' (ang)	Volume of unitcell (\AA^3)	Macrostrain	Crystallite size (nm)	Dislocation density	Average Crystallite Size (nm)
Cds (Pure)	111	26.68	3.36	0.06	5.82	197.24	0.016	2.11	0.222	2.29
	220	44.16	2.05	0.06	3.55	44.81	0.015	2.49	0.161	
	311	52.32	1.74	0.06	3.02	27.77	0.016	2.27	0.193	
Cds:Co (3%)	111	26.52	3.35	0.05	5.80	195.67	0.012	2.75	0.131	3.44
	220	43.8	2.05	0.04	3.56	45.20	0.009	3.54	0.079	
	311	51.9	1.76	0.03	3.05	28.57	0.008	4.01	0.061	

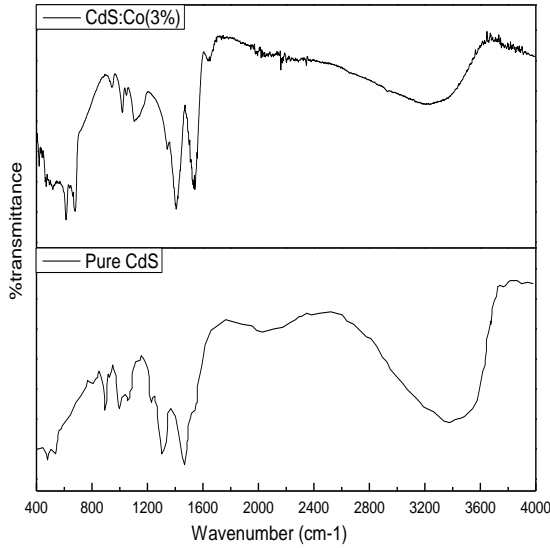


Figure 3 FTIR Analysis Of Pure CdS& CdS:Co (3%)

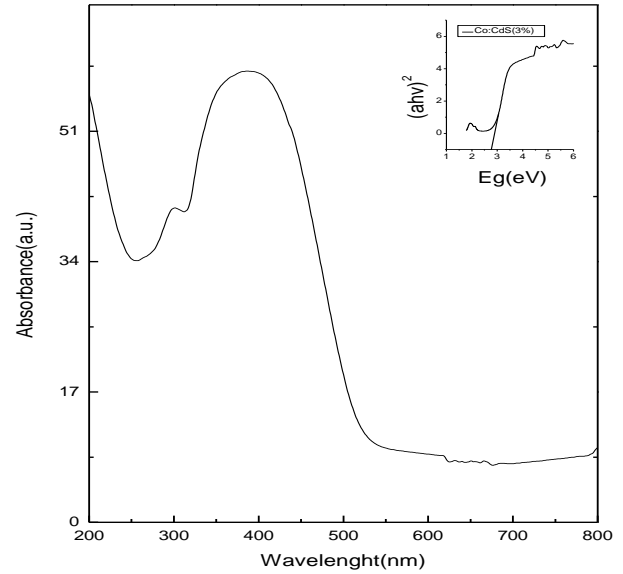


Figure 4 Absorption Spectra and Energy Band Gap of 3% Co-Doped CdS Nanoparticles

3.2 EDAX Analysis

Various techniques are used to study materials that are not made of regular stuff, like small-angle X-ray scattering, X-ray absorption fine structure (XAFS), X-ray diffraction, and X-ray photoelectron spectroscopy (XPS). These methods help scientists look closely at the surface or nearby areas of these special materials. To find out what elements are there and how much of each, energy-dispersive X-ray analysis (EDX) is used along with scanning electron microscopy (SEM). Think of SEM as taking pictures of the material with electron beams passing through it during the EDX analysis. This helps create maps of the elements present. Now let's focus on Co-doped CdS nanoparticles. Using EDX, images were taken of the surface, showing the presence of several elements in the nanoparticles (surface morphology). The EDX spectra, like a fingerprint, displays the elemental composition of the sample. In simple terms, the results of the EDX investigation tell us that there were balanced amounts of Cd, Co, and S in the synthesized samples. So, these techniques helped us understand

what's in these special materials and how they're put together.

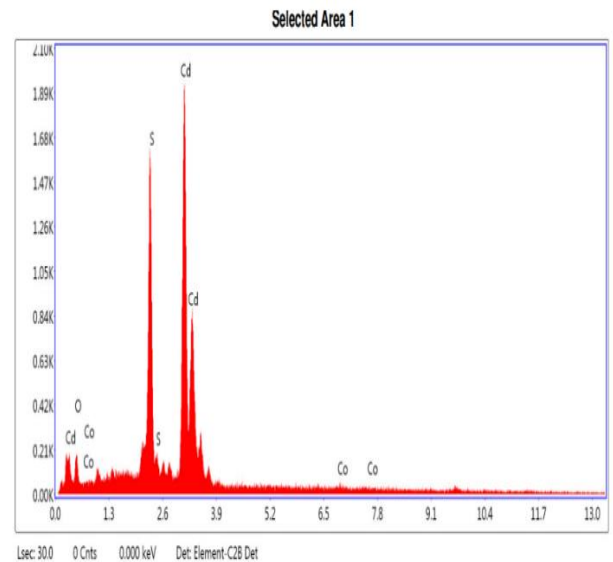


Figure 5 Energy Dispersive X- Ray Spectra (EDX) of CdS: Co (3wt%)

Table 2 EDX Compositional Analysis of the Prepared Samples

	Element	Weight %	Atomic %	Net Int.	Error %	K ratio
CdS:Co(3%)	O K	7.06	25.1	224.98	20.24	0.0098
	S K	21.65	38.4	524.16	4.47	0.2044
	CdL	70.38	35.62	660.35	2.83	0.6143
	CoK	0.91	0.88	6.22	58.56	0.0092

The spectra obtained through Energy-Dispersive X-ray Analysis (EDAX) for Co-doped CdS nanoparticles at concentrations (3%) in the preceding figures confirm the absence of any additional contaminants or impurities in the samples. The findings undeniably show that with increasing concentrations of Co, the intensity of the Co peaks noticeably increases.

Conclusion

The microwave-assisted solvothermal approach was used to create cobalt-doped cadmium sulphide semiconductor nanoparticles (CdS: Co) NPs at concentrations of Co (3%). For pure CdS, the XRD spectra display three main peaks at $2\theta = 26.68^\circ$, 44.16° , and 52.9° . After doping (3%) the XRD spectra display three main peaks at $2\theta = 26.52^\circ$, 43.8° , and 51.32° . Modest alterations have been noted in 2θ for Co doping levels of 3% in CdS NPs. The peaks point to the samples' cubic structure and correlate to the (1 1 1), (2 2 0), and (3 1 1) planes. The sizes of the nanoparticles, which are 2.29 nm, 3.64 nm, for pure and Co (3%) doped CdS respectively, were determined using the FWHM and Debye Scherer equation. The substitution of Co²⁺ ion for Cd²⁺ ion may be the cause of the decrease in nanoparticle size observed in the Co-doped CdS sample as concentration rises. The difference in the ionic radii of Cd²⁺ (0.98 Å) and Co²⁺ (0.72 Å) show that when the concentration of Co-doped CdS increases, the

lattice constant falls. The peak at 3646 cm⁻¹ in the higher energy area of the 400–4000 cm⁻¹ FTIR spectra is attributed to the O–H stretching of absorbed water on the surface of CdS [12-15]. Its bending vibration confirms the existence of water. Using HRTEM, the size of the produced nanoparticles was examined. Additionally, it confirms the sample's nanocrystalline structure. For 3% Co-doped CdS, the average size of randomly chosen nanoparticles is determined.

References

- [1]. Amira Ben Gouider Trabelsi, et.al, Journal of materials research and Technology, 21, 3982-4001(2022) <https://doi.org/10.1016/j.jmrt.2022.11.002>
- [2]. S. K. Choubey, A. Kaushik, K. P. Tiwary, Chalcogenide Letters, 15(3) 125(2018)
- [3]. Ibrahim Khana, Khalid Saeed, Idrees Khan Arabian, Journal of Chemistry, 12(7) 908(2019) <https://doi.org/10.1016/j.arabjc.2017.05.011>
- [4]. K. P. Tiwary, F. Ali, R. K. Mishra, S. Kumar, K. Sharma, Digest Journal of Nano-materials and Biostructures, 14 (2) 305(2019).
- [5]. Christine Barglik-Chory, Christian Remenyi, Cristina Dem, Michael Schmitt, et.al PCCP 5(8)1639(2003); <https://doi.org/10.1039/b300343d>

- [6]. Pratibha R. Nikam, et.al Journal of Alloys and Compounds.689394(2016)
- [7]. K P Tiwary, F. Ali, R K Mishra, S K Choubey, K Sharma, Journal of Ovonic Research, 16(4)234(2020)
- [8]. Uma Shankar Patel, Rakesh Kumar Ahirwar, Anjali Bhatt, B. S. Arya, AIP Publishing,2100(1) 2019; <https://doi.org/10.1063/1.5098719>
- [9]. A.Gadalla, M. Almokhtar, A. N. Abouelkhir, Chalcogenide Letters, 15(4), 207(2018).
- [10]. Ankit Goyal, Vinay Sharma, Abhishek Sharma, Ravi Agarwal, K.B. Sharma, S.L. Kothari, J.Nano- Electron. Phys.3(1) 254(2011).
- [11]. Anshu Dandia, Vijay Parewa, Kuldeep S. Rathore, Catalysis Communications 28 90(2012); <https://doi.org/10.1016/j.catcom.2012.08.020>
- [12]. H K Jun, M A Careem and A KArif, Renew. Sust. Energ. Rev. 22 148(2013);
- [13]. Shweta Chaure, Materials Research Express, 6 2(2018). <https://doi.org/10.1088/2053-1591/aad4e1>
- [14]. S. K. Choubey, K. P. Tiwary, Digest Journal of Nanomaterials and Biostructures, 11(1)33(2016).
- [15]. R. Ranjan, C. M. S. Negi, K. P. Tiwary, Chalcogenide Letters,20(4), 251(2023); <https://doi.org/10.15251/CL.2023.204.251>